www.ptcer.pl/mccm

MATERIAŁY CERAMICZNE /CERAMIC MATERIALS/, 62, 3, (2010), 335-341

Design of Alumina-Zirconia Nanocomposite Powders for Implants Development

Laura Montanaro[1]*, Jérôme Chevalier[2], Valentina Naglieri[1], Lucile Joly-Pottuz[2]

[1] Politecnico di Torino, Department of Materials Science and Chemical Engineering
LINCE Lab R.U. INSTM PoliTO, Torino, Italy
[2] University of Lyon, INSA de Lyon, MATEIS Lab., UMR CNRS 5510, Villeurbanne, France
*e-mail: laura.montanaro@polito.it

Abstract

A 95 vol.% alumina – 5 vol.% zirconia composite powder was produced following a simple surface modification procedure, starting from a zirconium chloride aqueous solution and a commercial, ultra-fine α-alumina powder. The evolution of phases as well as of the nano-microstructure was followed as a function of powder heat-treatments prior to sintering, in order to develop a preliminary "nano-powder engineering" approach, in view of a controlled tailoring of the microstructural features of the dense materials.
Keywords: Nanopowders, Nanocomposite, Al_2O_3, ZrO_2, Biomedical applications

PROJEKTOWANIE NANOKOMPOZYTOWYCH PROSZKÓW TLENKÓW GLINU I CYRKONU NA POTRZEBY ROZWOJU IMPLANTÓW

Proszek kompozytowy o składzie 95 % obj. Al_2O_3 – 5 % obj. ZrO_2 wyprodukowano postępując zgodnie z prostą procedurą modyfikowania powierzchni, wychodząc z roztworu wodnego chlroku cyrkonu i handlowego ultra-drobnego proszku α-Al_2O_3. Ewolucję składu fazowego, a także nano-mikrostruktury śledzono jako funkcję obróbki cieplnej proszku poprzedzającej spiekanie, aby rozwinąć problem wstępnej "inżynierii nanoproszku", biorąc pod uwagę kontrolowane kształtowanie cech mikrostrukturalnych gęstych materiałów.
Słowa kluczowe: nanoproszki, nanokompozyty, Al_2O_3, ZrO_2, zastosowania biomedyczne

1. Introduction

An overriding guideline in the design of innovative materials and devices for orthopaedics is the request of high-performance and long-lasting implants through a suitable combination of mechanical and tribological properties and in vivo stability [1, 2].

Zirconia toughened alumina (ZTA) composites are now promising candidates for replacing alumina and zirconia monoliths, since they offer a relevant increase of the crack growth resistance [2, 3]. This advantageous feature can lead to a higher reliability and a lower risk of failure, needed for reaching a component lifetime longer than the mean life expectancy of the patients, as well as to an improvement in the versatility of the component design for a better fit of the human body configuration. An additional advantage can result by the development of nano-structured composites in which zirconia nano-grains are homogeneously distributed into a fine and dense alumina matrix. Zirconia can be stabilized in the tetragonal form by a size effect, without yttria addition, thus avoiding the possible ageing promotion induced by the oxygen vacancies created by Y^{3+} addition [4]. However, it has been recently demonstrated that processing and microstructure development play a key role in optimising the mechanical properties and reliability of ZTA materials [5].

A simple and successful procedure has been set-up to develop alumina-based composite powders, able to produce fully dense materials by pressureless sintering, in which a nano-sized second phase is homogeneously distributed into a micronic or sub-micronic alumina matrix, mainly in inter-granular position [6]. Such apromising procedure can be easily transferred to a large-scale production, exploiting several commercial alumina powders as a matrix and using common inorganic salts as precursors of the second phase. However, to achieve a complete control of the procedure and therefore to perform a suitable tailoring of the final microstructure in order to meet the major constraints of any specific application, a deeper investigation of the powder evolution during thermal pre-treatment prior sintering is needed as a preliminary step for a knowledge-based approach to an effective nano-powder engineering.

This paper deals with the selected tools and related information collected during this cognitive path and the possible scenario of crystallization and growth of zirconia nano-grains

onto α-alumina grains surface, through the definition of the involved mechanisms and of the ways to better manage them.

2. Experimental

A commercial α-alumina powder (TM-DAR TAIMICRON, supplied by Taimei Chemicals Co., Japan, Fig. 1) was used to prepare a 95 vol.% alumina - 5 vol.% zirconia nanocomposite. It is characterized by a mean particle size of 150 nm [7].

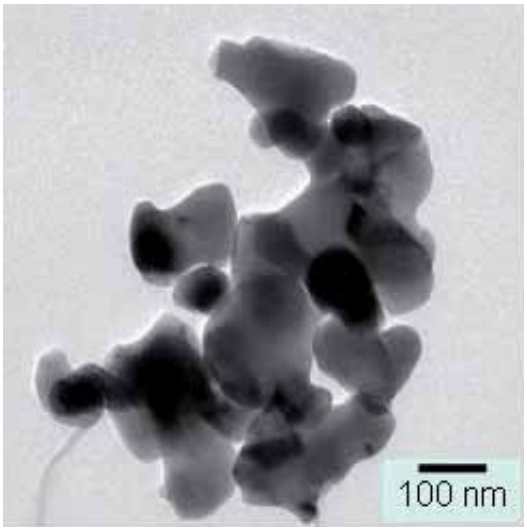

Fig. 1. TEM image of the as-received α-alumina.

Firstly, the alumina powder was dispersed in distilled water under magnetic stirring for several hours. Then, an aqueous solution of zirconium chloride (0.38 M) was dropwise added to the alumina slurry (solid content of 33 wt%) in a suitable amount to develop the above composition after calcination. After homogenization under stirring for 1 h, the doped suspensions were diluted down to 4 wt% and spray dried (Mini Spray Dried Büchi B-290), in order to avoid salt segregation. More details about the above procedure have been recently published [6]. After a pre-treatment at low temperature (600°C for 1 h) to induce the thermal decomposition of the by-products, set-up on the ground of thermogravimetric-differential thermal analyses (TGA-DTA, SETARAM TG-DTA 92) performed up to 1000°C, the powders were uniaxially pressed at about 300 MPa and pressureless sintered at 1500°C for 3 h, yielding a promising microstructure made of zirconia nano-grains, homogeneously distributed into a micronic alumina matrix at intergranular positions (Fig. 2).

For a deeper knowledge of the zirconia nucleation and growth on alumina grains surface, in view of achieving a knowledge-based control of the final microstructure, in this work the dried composite powders were first treated at various temperatures in the range 400–1000°C (heating rate of 5°C min^{-1}), holding them in temperature for times ranging from 1 up to 20 h. Calcined powders were then submitted to X-Ray Diffraction (XRD, Philips PW 1710, Cu anticathode) to follow phase evolution as a function of temperature and time. Small samples of powder were also submitted to isothermal treatments, by quickly plunging into a furnace, already brought to and kept at a steady temperature (*i.e.*, 500°C, 600°C, 800°C, 1000°C, respectively), and then holding them in temperature for 1, 2, 5, 15, 30 min, 1, 2, 3, 6, 9, 12, 24 h,

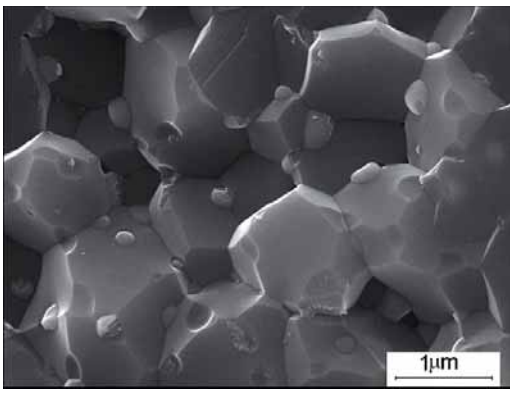

Fig. 2. SE-ESEM image of the alumina-zirconia sintered material [6].

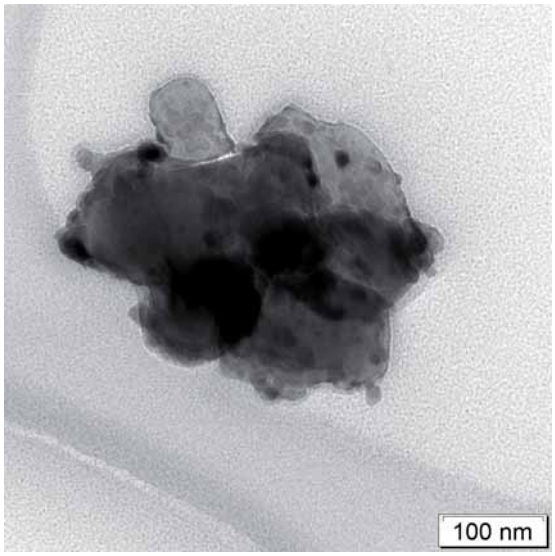

a)

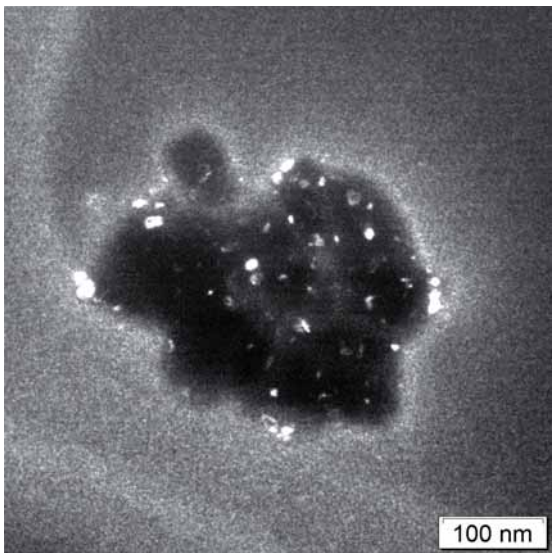

b)

Fig. 3. TEM images of the 95 vol.% Al_2O_3 - 5 vol.% ZrO_2 powder after treatment at 800°C for 1 hr: a) bright field image, b) dark field image.

respectively. Conventional XRD analyses (XRD, Philips PW 1710, Cu anticathode, λ_{cu} of 1.54060 Å, 2θ range of 24–33°) were carried out on isothermally-treated samples. The average crystallize size was calculated by the line-broadening method, using Scherrer's equation. The area of the main

zirconia peak (101) was measured and used to calculate a crystallinity degree index. Therefore, the crystalline fraction *f* of each sample was calculated as the ratio between the area of its main zirconia peak and that presented by a sample in which zirconia was fully crystallized.

Transmission Electron Microscopy (TEM; LEO 912 instrument, operating at 120 kV accelerating voltage) observations of the same powders allowed the authors to study the nucleation and growth of zirconia crystallites on alumina grains surface. Specimens were prepared by slow evaporation of a drop of the powder suspension in ethanol, deposited onto perforated carbon-covered copper grids. Images were collected both in the bright field (BF, Fig. 3a) and dark the field (DF, Fig. 3b) mode. In the latter case, images were obtained with the objective aperture positioned on the first zirconia ring of the diffraction pattern, at which the objective aperture only selects the electrons which are in Bragg conditions for zirconia crystallites, so that only zirconia crystallites are illuminated as white dots.

Furthermore, a specific feature available on LEO microscope which allows us to perform annular dark field (ADF) images in the TEM mode was used. This is made possible by rotating the diffraction pattern through the small objective aperture so that the whole selected ring is used to give the DF image. Thus, all the zirconia crystallites in Bragg conditions can be imaged in the sample, allowing a more precise determination of their size distribution through numerical analyses performed on DF low magnification images. The evolution of zirconia crystallites size as a function of treatment temperature and time was then followed on the differently calcined samples.

High-Resolution Transmission Electron Microscopy (HR-TEM) was also performed on selected thermally treated powders by using a JEOL 2010 F Microscope under 200 kV Voltage.

High temperature-XRD analyses were also performed, by means of a Bruker diffractometer (Cu anticathode, 2θ range of 24.2–38.3°), heating the sample at a fixed temperature rate (temperature ramps of 1.5°C min^{-1}, 4.2°C min^{-1}, 5.6°C min^{-1}, 30°C min^{-1} respectively, were investigated) up to 500°C, 600°C, 800°C, 1000°C and 1200°C, respectively, followed by an isotherm soaking at the maximum temperature for 12 h.

Finally, tetragonal-ZrO_2 meta-stabilization was pursued just by a "size effect", based on the nanometric dimensions of the second phase grains present in the sintered materials. A complementary doping with the yttrium chloride solution could be expected to affect phase purity, since the described preparation procedure has been also successfully applied for producing alumina-YAG (yttrium aluminium garnet) composites in the past [6]. However, zirconia stabilization with Y_2O_3 addition can be effectively performed on the ground of the recent work [8], in which tri-phasic composites (alumina-zirconia-YAG) were developed by exploiting the above procedure, *i.e.*, by adding a mixed aqueous solution of zirconium and yttrium chlorides to the α-alumina powder. In that case, a preferential diffusion of yttrium ions into ZrO_2 lattice was demonstrated, up to obtain a fully stabilized zirconia in the cubic phase, before starting to yield yttrium aluminates, and finally YAG.

At the same time, we decided to perform the present investigation without yttria addition, since it is known [4] that yttrium, as a trivalent ion, induces oxygen vacancies formation, able to promote hydroxyl groups diffusion into the zirconia lattice, thus actively contributing to ageing. Also this second point strengthens the need of a rigorous control of the microstructural features, not only in terms of mean crystallite size, but also for avoiding any localized grain growth and consequent tetragonal to monoclinic transformation.

3. Results and discussion

Tetragonal ZrO_2 started to crystallize from the amorphous by-products yielded by the thermal decomposition of the salt precursor, as confirmed by conventional XRD performed on the powder after calcination at 500°C.

In Fig. 4a detail of the diffraction patterns collected on powders calcined at 500°C for increasing times is reported, showing the evolution of the main peak of tetragonal zirconia, which was already detectable after 5 min. soaking at this temperature. The peak area, proportional to the amount of crystallized zirconia, increased as a function of time, reflecting the evolution of the second phase during the isothermal treatments, as detailed below.

Regarding the zirconia growth rate during isothermal treatments, evaluated from XRD patterns, just a slight increase of the mean grain size was observed at low treatment temperature, while at higher temperatures crystallite growth was more significant.

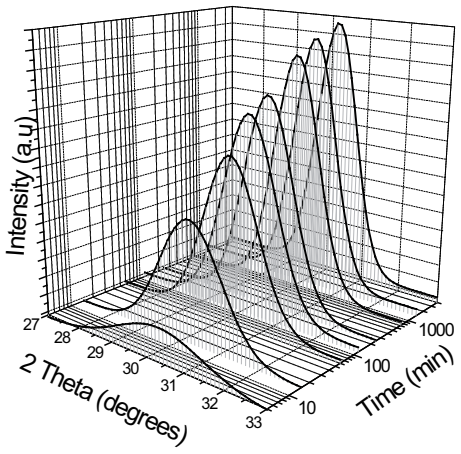

Fig. 4. Evolution of the main diffraction peak of tetragonal zirconia in powders calcined at 500°C for increasing times.

The same trend was observed performing treatments upon continuous heating; in fact, Fig. 5 shows the evolution of crystallite size as a function of temperature, fitting all the points collected during the several heatings at various heating rates in HT-XRD apparatus. As expected, the mean crystallite size increased with the treatment temperature, even if the growth rate was very low between 500°C and 800°C, while an abrupt increase in crystallization rate was observed at higher temperatures. All the collected crystallite size data were fitted by a growth exponential function, reaching a good correlation factor (R^2 = 0.95).

This trend also supported the choice, previously stated, of a low-temperature pre-treatment of the powder prior sintering (600°C for 1 h [6]), so that the mass loss of about 24 % recorded by thermal analysis and imputable to the

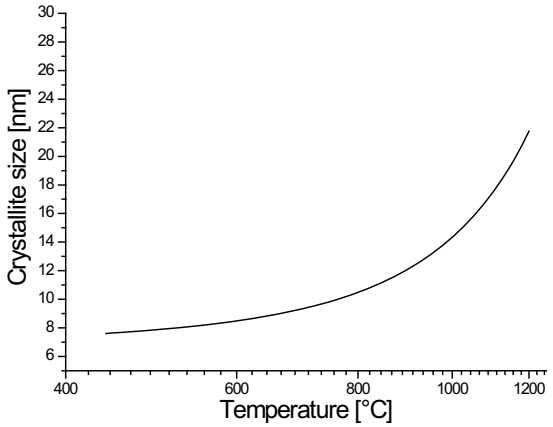

Fig. 5. Evolution of the crystallites size vs. temperature (log scale).

The mean zirconia crystallite sizes, measured by the above technique, were 9, 11, 17 and 25 nm for the samples treated at 500, 600, 800 and 1000°C, respectively (Figs. 6 a, b, c and d).

TEM and HR-TEM observations (Figs. 7a and 7b) allowed us to draw out more precise details on crystallization path.

After drying and thermal decomposition of the precursor, the alumina grains were enveloped by an amorphous layer, a few tens of nanometer in thickness, in which zirconia crystallites started to nucleate.

The almost round-shaped crystallites of a few nanometers in size appeared almost completely detached from the surface and related crystallographic terminations of the α-alumina grains. Thus, the images supported the hypothesis of a homogeneous nucleation of zirconia.

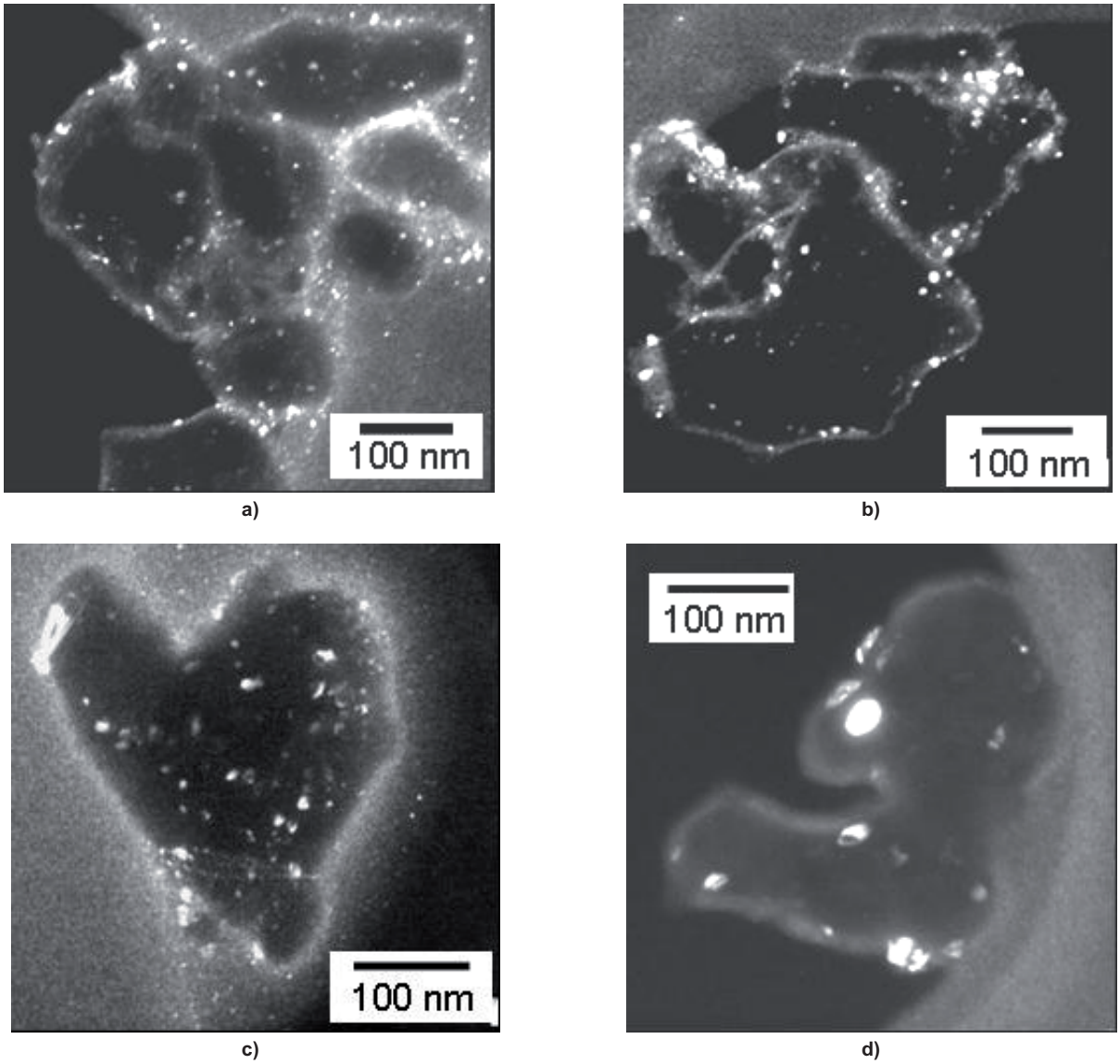

Fig. 6. Dark Field - TEM images of the composite powders treated at: a) 500°C, b) 600°C, c) 800°C, d) 1000°C for 1 h.

by-products decomposition could be completely recovered without inducing relevant crystallite growth.

Crystallite growth followed by TEM observations of differently calcined powders allowed the authors to confirm the above statements.

Increasing treatment temperature, the thickness of the amorphous layer progressively decreased (Figs. 8a and 8b) due to the increase of the crystallised fraction of zirconia (Fig. 9).

Another interesting evolution can be pointed out observing the powder calcined at temperatures higher than 500°C

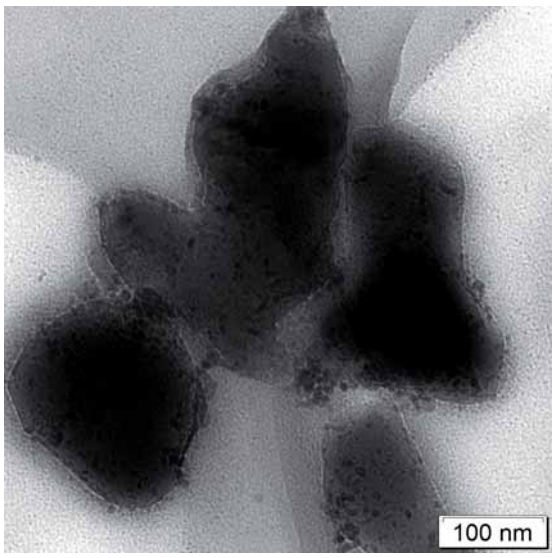

a)

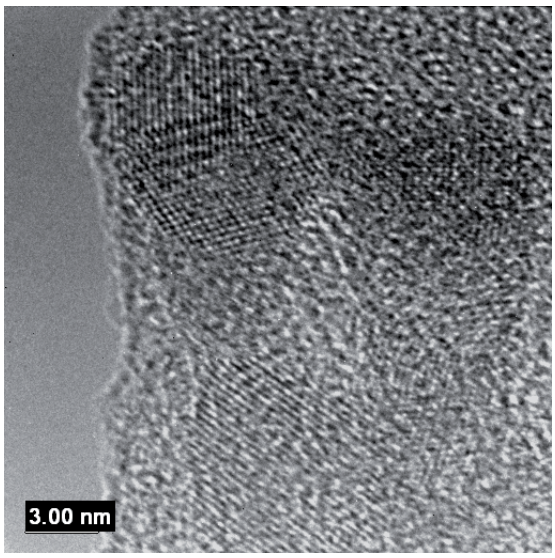

b)

Fig. 7. TEM (a) and HR-TEM (b) images of the composite powder treated at 500°C for 1 h.

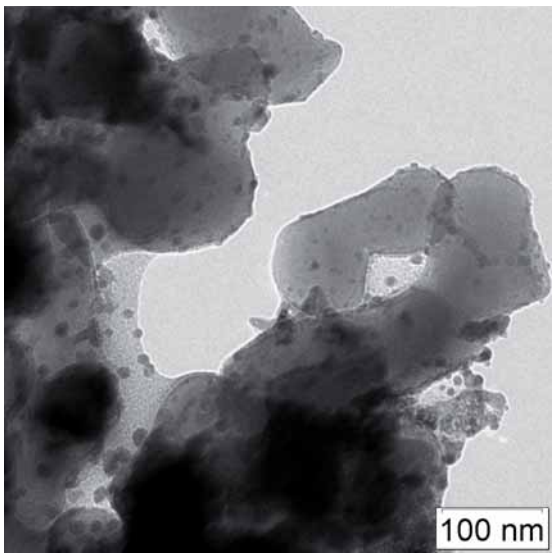

a)

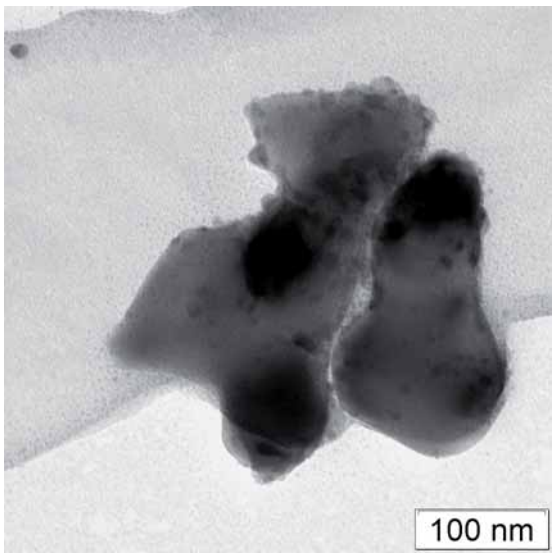

b)

Fig. 8. TEM images of the powder calcined at: a) 600°C and b) 1000°C for 1 h.

by HR-TEM (Figs. 10a and 10b).

As the temperature increased and the thickness of the amorphous layer decreased, the zirconia crystallites were forced to progressively approach the α-alumina grains surface.

A gradual decrease of the contact angle was appreciable up to the higher treatment temperatures at which a grain boundary between the two phases was finally developed.

In addition, a particular behaviour was observed if prolonged isothermal treatments were performed at low-medium temperature, at which a still relevant thickness of amorphous layer is present on the grains surface. In fact, it was observed that locally, where allowed by the alumina aggregates morphology, discrete pockets were formed, in which the amorphous phase is preferentially drained (Figs. 12a and 12b).

Into these pockets many small zirconia crystallites were dragged by the amorphous phase flow and forced to approach each other. This behaviour was not generalised on the whole alumina surfaces, as it can be clearly observed

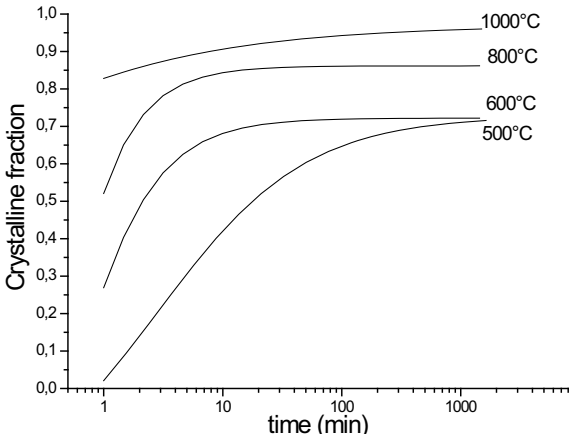

Fig. 9. Zirconia crystalline fraction vs. time (log scale), for the powder submitted to isothermal treatments at different temperatures.

by TEM, since many other zirconia grains remained almost isolated on the alumina grains surface. However, this local phenomenon could lead, during the following high-temper-

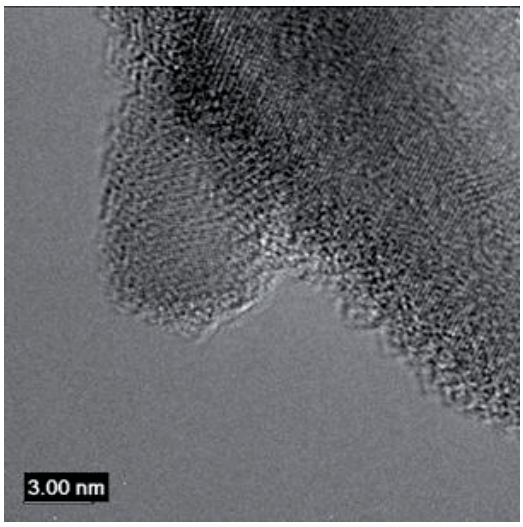

a)

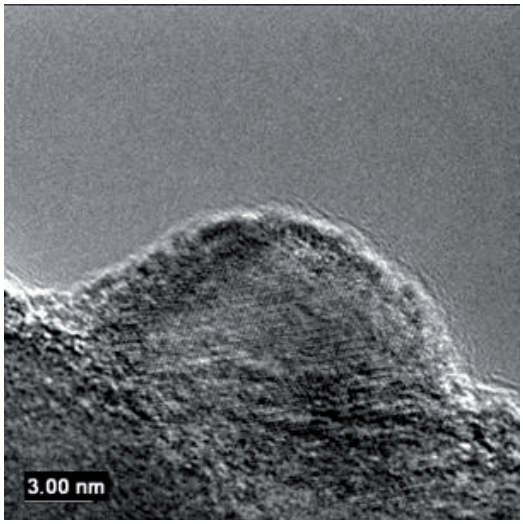

b)

Fig. 10. HR-TEM images of the powder treated at: a) 600°C, b) at 1000°C for 1 h.

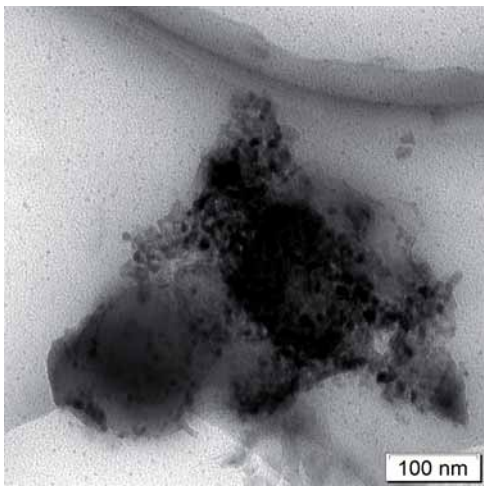

a)

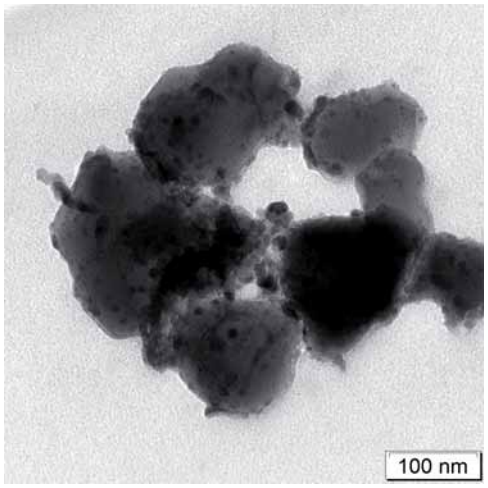

b)

Fig. 11. TEM images of the powder calcined at: a) 500°C and b) 600°C for 10 h.

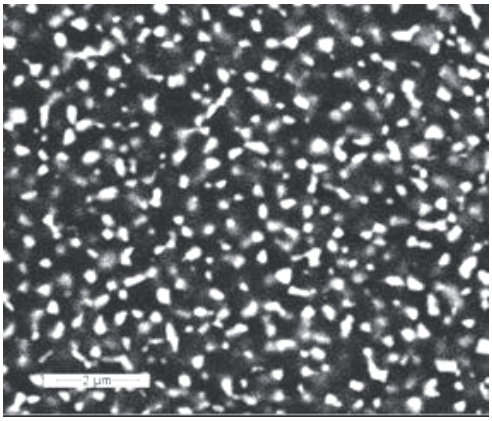

a)

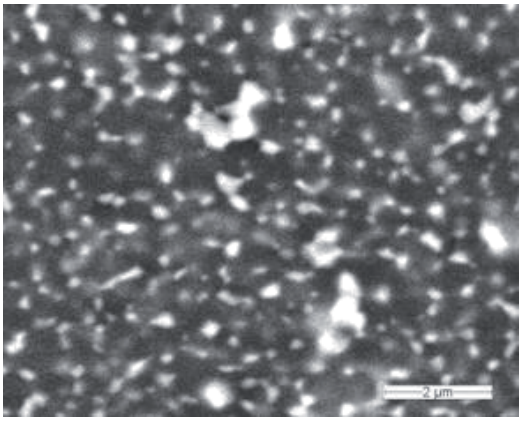

b)

Fig. 12. SEM microstructure of materials sintered at 1500°C for 3 h, obtained by a powder pre-treated at 600°C for: a) 1 h and b) 20 h.

ature treatments, to the coalescence of the nano-grains and to a subsequent, undesired growth of some zirconia grains, inducing microstructural heterogeneity and risk of phase transformation. On the same time, the not dragged grains remained surrounded by a lower amount of amorphous phase, thus limiting their subsequent growth. As a consequence, a more heterogeneous grain size distribution of the second phase should be expected. A systematic investigation is now in progress to support the above hypothesis, *i.e.*, a prolonged treatment at a low-medium temperature can induce grain coalescence and less homogeneous growth, by comparing the microstructures of sintered materials obtained by pow-

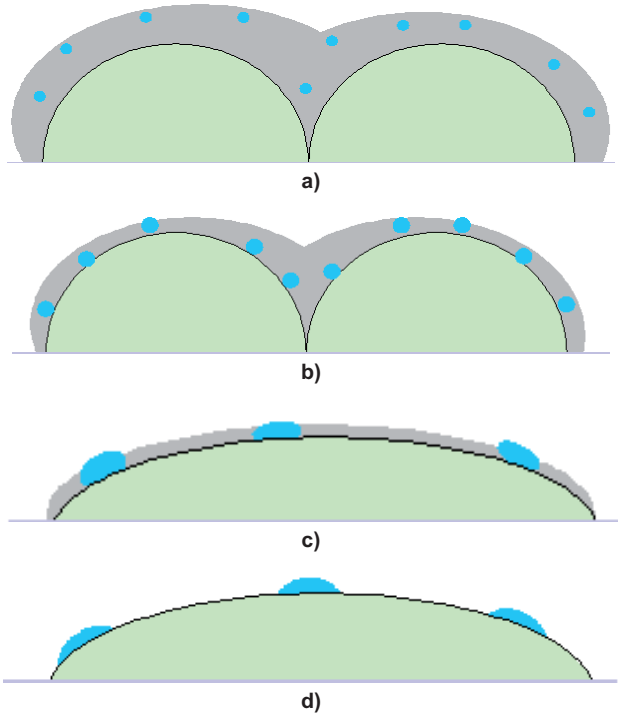

Fig. 13. A possible scenario for the nucleation and growth of zirconia nano-crystals on the surface of the α-alumina grains.

ders pre-treated at 600°C for different times (from 1 to 20 h, for instance; Figs. 12a and 12b). A preliminary evidence of a more heterogeneous microstructure was found in the case of sintered materials obtained by powders pre-calcined at 600°C for longer times.

4. Conclusions

From the above experimental results, a possible scenario for nucleation and growth of zirconia nano-grains onto an α-alumina powder can be drawn out, in particular two different paths can be described, the former being desired in view of a control of the final microstructure (Fig. 13), the latter to be avoided since potentially hindering the achievement of a homogeneous distribution of nano-grains size (Fig. 14).

In the first case, a homogeneous nucleation was observed into the amorphous layer yielded by the precursor thermal decomposition, wrapping the alumina grains. By increasing the calcination temperature, the layer became thinner and thinner, since crystallization proceeded and the zirconia crystallites were forced to approach the alumina grains, to adapt themselves to their surfaces and finally to develop their final grain boundaries.

However, if the calcination time was prolonged to many hours in order to promote the amorphous layer disappearance at a low temperature, at which crystal growth is less favourable, a draining of a part of the amorphous phase in discrete pockets was observed, promoted by local alumina aggregate morphology, and some zirconia nano-grains were consequently dragged and forced to approach each others.

This phenomenon induced a favourable condition to grain coalescence and subsequent growth, potentially leading to a local, uncontrolled microstructural development.

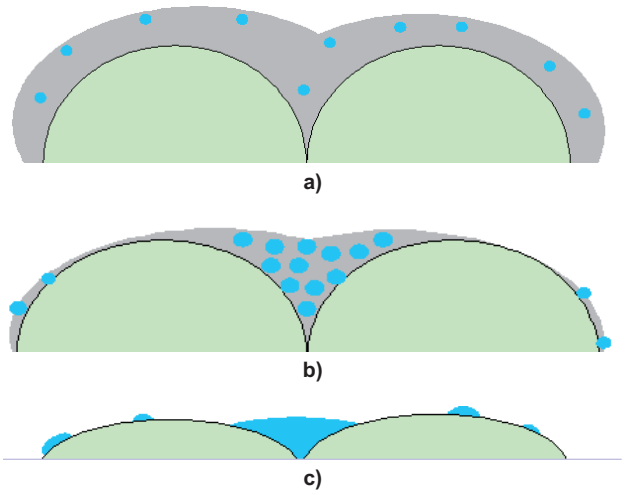

Fig. 14. A scheme illustrating an undesired microstructural evolution promoted by prolonged isothermal treatments at low-medium temperature.

Acknowledgments

The CLYM (Centre Lyonnais de Microscopie) is gratefully acknowledged for the access to the Transmission Electron Microscope.

The authors thank the European Commission for partially supporting this work in the framework of Integrated Project "NANOKER-Structural Ceramic Nanocomposites for top-end Functional Applications", contract no: NMP3-CT-2005-515784.

References

[1] Rahaman M.N., Yao A., Sonny Bal B., Garino J.P., Ries M.D.: „Ceramics for Prosthetic Hip and Knee Joint Replacement", J. Am. Ceram. Soc., 90, (2007), 1956-1988.
[2] Chevalier J.: „What a future for zirconia as a biomaterial?", Biomaterials, 27, (2006) 535-543.
[3] De Aza A.H., Chevalier J., Fantozzi G., Schehl M., Torrecillas R.: „Crack growth resistance of alumina, zirconia and zirconia toughened alumina ceramics for joint prostheses", Biomaterials, 23, (2002), 937-945.
[4] Chevalier J., Cales B., Drouin J.M.: „Low temperature Aging of Y-TZP Ceramics", J. Am. Ceram. Soc., 82, (1999), 2150-2154.
[5] Gutknecht D., Chevalier J., Garnier V., Fantozzi G.: „Key role of processing to avoid low temperature ageing in alumina-zirconia composites for orthopaedic application", J. Eur. Ceram. Soc., 27, (2007), 1547-1555.
[6] Palmero P., Naglieri V., Chevalier J., Fantozzi G., Montanaro L.: „Alumina-based nanocomposites obtained by doping with inorganic salt solution: application to immiscible and reactive system", J. Eur. Ceram. Soc., 29, (2009), 59-66.
[7] http://www.taimei-chem.co.jp
[8] Naglieri V., Palmero P., Montanaro L.: „Preparation and characterization of alumina-doped powders for the design of multi-phasic nano-microcomposites", J. Therm. Anal. Cal., 97, (2009), 231-237.

♦

Received 1 March 2010; accepted 5 May 2010